

MR signal change in venous thrombus relates organizing process and thrombolytic response in rabbit

Yasuyoshi Kuroiwa^{a,b,d}, Atsushi Yamashita^b, Tosiaki Miyati^d, Eiji Furukoji^c,
Misaki Takahashi^b, Toshiya Azuma^c, Hiroshi Sugimura^c, Taketoshi Asanuma^e,
Shozo Tamura^c, Keiichi Kawai^{d,f}, Yujiro Asada^{b,*}

^aDepartment of Radiological Technology, Koga General Hospital, Miyazaki, Japan

^bDepartment of Pathology, Faculty of Medicine, University of Miyazaki, Miyazaki, Japan

^cDepartment of Radiology, Faculty of Medicine, University of Miyazaki, Miyazaki, Japan

^dDivision of Health Sciences, Graduate School of Medical Science, Kanazawa University, Ishikawa, Japan

^eDepartment of Veterinary Sciences, Faculty of Agriculture, University of Miyazaki, Miyazaki, Japan

^fBiomedical Imaging Research Center, University of Fukui, Fukui, Japan

Received 21 October 2010; revised 18 April 2011; accepted 22 April 2011

Abstract

Venous thrombus is subsequently organized and replaced by fibrous connective tissue. However, the sequential changes in venous thrombi are not reliably detected by current noninvasive diagnostic techniques. The purpose of this study is to reveal whether magnetic resonance (MR) can detect venous thrombus, define thrombus age and predict thrombolytic responses. Thrombus in the rabbit jugular vein was imaged with a 1.5-T MR system at 4 h and at 1, 2 and 4 weeks using three-dimensional (3D) fast asymmetric spin echo T2-weighted (T2W) and 3D-gradient echo T1-weighted (T1W) sequences. The jugular veins were histologically assessed at each time point. Magnetic resonance imaging (MRI) was also performed *in vivo* before and 30 min after tissue plasminogen activator (t-PA) administration. The thrombi in MRI were comparable in size to histological sections. The signal intensity (SI) of thrombi at 4 h was heterogeneously high or low on T2W or T1W images, respectively. The SI of thrombi on T2W images decreased time-dependently, but increased on T1W images at 1 and 2 weeks. Morphological analysis showed time-dependent decreases in erythrocyte, platelet and fibrin areas and time-dependent increases in smooth muscle cell, macrophage, collagen and iron areas. The t-PA administration significantly decreased thrombus volume at 4 h but not at 1, 2 and 4 weeks. Venous thrombosis can be reliably and noninvasively detected by MRI. Measurement of SI might support assessments of thrombus age and thrombolytic response.

© 2011 Elsevier Inc. All rights reserved.

Keywords: Magnetic resonance imaging; Signal intensity; Thrombolysis

1. Introduction

Deep venous thrombosis (DVT) and pulmonary embolism, which are collectively termed venous thromboembolism, comprise a major medical concern in Europe and North America, especially among the elderly [1]. Although they can arise in veins of the limbs as well as in renal, mesenteric, splenic, portal or cerebral veins, they mainly develop in the deep veins of the lower legs. Venous

thrombus initially consists of erythrocytes, platelets and fibrin [2,3] that become organized and replaced with fibrous connective tissue [4,5]. However, sequential changes in venous thrombi are not reliably detected by current noninvasive diagnostic techniques, such as ultrasonography and computed tomography [6].

Thrombolytic therapy can be effective against DVT, resulting in rapid clot lysis, less impaired venous hemodynamics and reduced long-term morbidity from chronic venous insufficiency as compared with anticoagulant treatment alone [7,8]. Because thrombolytic therapy results in a substantial increase in risk of bleeding compared with anticoagulant treatment alone, to predict the outcome of

* Corresponding author. Tel.: +81 985 85 2810; fax: +81 985 85 7614.
E-mail address: yasada@fc.miyazaki-u.ac.jp (Y. Asada).

thrombolytic therapy in patients with DVT is of particular concern. To clinically evaluate the age of thrombus and to predict responses to thrombolytic therapy are difficult.

Magnetic resonance imaging (MRI) for DVT was introduced in the early 1990s, and it is more accurate than conventional venography and ultrasonography [9–12]. A variety of techniques have been described, including a two-dimensional (2D) time-of-flight (TOF) angiography with arterial flow suppression, three-dimensional (3D) T1-weighted prepared gradient echo sequence with fat saturation and a contrast-enhanced T1 fast field echo [13]. Although an animal study has advocated using MRI to detect venous thrombosis, MR images and age-related changes have not been adequately characterized [14]. Magnetic resonance imaging generates high tissue contrast in terms of biophysical and biochemical parameters. We therefore examined the ability of MRI to detect venous thrombosis, define thrombus age and predict thrombolytic responses in a rabbit model of venous thrombosis.

2. Materials and methods

2.1. Venous thrombus formation in rabbit jugular vein

The Animal Care Committees of our institutions approved the animal research protocols, which conformed to the *Guide for the Care and Use of Laboratory Animals* published by the US National Institutes of Health.

Table 1 shows the protocol in this study. Thirty-nine male Japanese white rabbits weighing 2.5 to 3.0 kg were fed with a conventional diet. All surgical manipulations proceeded under aseptic conditions and general anesthesia induced via an intravenous (iv) injection of pentobarbital (25 mg/kg, body weight). Thrombi were generated in the right jugular veins by a combination of endothelial denudation induced by inserting a 4F balloon catheter (Edwards Lifesciences, Irvine, CA, USA) into the right jugular vein and vessel ligation (blood stasis) [15] achieved by ligating 12 mm of the jugular vein. The jugular veins ($n=6$ each) were visualized by MRI at 4 h and at 1, 2 and 4 weeks after the procedure, and images were analyzed at 3-mm intervals. At each time point, rabbits ($n=3$ each) were injected with heparin (500 U/kg, iv) and then sacrificed with an overdose of pentobarbital (60 mg/kg, iv) for histological analysis. The animals were perfused with 50 ml of 0.01 mol/L phosphate-buffered saline and then perfusion-fixed with

4% paraformaldehyde for histological and immunohistochemical evaluation.

The jugular veins were also visualized by MRI before and 30 min after an infusion of tissue plasminogen activator (t-PA, 600,000 U/kg/h) at 4 h and at 1, 2 and 4 weeks after the procedure to determine the effects of thrombolytic therapy ($n=6$ each).

2.2. MR imaging

Four hours and 1, 2 and 4 weeks after thrombus formation, the rabbits were anesthetized and placed in the left decubitus position in a 1.5-T superconductive magnet unit (Excelart Vantage XGV Power Plus Package, Toshiba Medical Systems, Tokyo, Japan) using a 200-mm quadrature transmitter/receiver coil. The localizer consists of fast, multislice, multistack (axial, sagittal and coronal images) segmented field echo localizer scans of the jugular vein (repetition time, 160 ms; echo time, 5 ms; flip angle, 30°; slice thickness, 3 mm; field of view, 200×200 mm; matrix, 128×256). From axial images of the jugular vein, a second coronal scout with a reduced slice thickness (1 mm) was obtained along its major axis. The ligated sutures, trachea or the carotid artery served as a landmark to position MR cross-sectional images of the jugular vein. Three-dimensional fast asymmetric spin echo (FASE) T2-weighted images (T2WIs) with fat suppression were acquired with a repetition time (TR) and echo time (TE) of 2000/60 ms and 120 ms, and 3D-gradient echo T1-weighted images (T1WIs) with fat suppression were acquired with a TR, TE and flip angle (FA) of 38 ms, 5 ms and 20° and 40°. Further MR imaging parameters included the following: field of view, 120×120 mm; matrix, 256×256 (zero-filled interpolated to 512×512 to reduce partial-volume effects in imaging pixels) [16]; a 3mm slice thickness; and one signal average. The voxel size of the MR images of jugular vein thrombi was 0.47×0.47×3 mm.

2.3. Image and data analysis

The MR images ($n=3$ per vein) were further analyzed using a Macintosh computer and matched with corresponding histopathological sections of jugular vein specimens. Cursors for regions of interest defined by one observer were placed within the thrombus to measure cross-sectional area, signal intensity (SI), and T1 and T2 relaxation times. The cross-sectional area of the thrombus was determined for both MR images by manual tracing using Image J (US National Institutes of Health, Bethesda, MD, USA). To determine MR SI changes in the organizing processes of venous thrombus, we assessed the intrinsic MR properties of thrombi by measuring the SI relative to the reference muscle using the formula $SI (\%) = 100 \times (SI_{\text{thrombus}} / SI_{\text{muscle}})$ on the T2WIs and T1WIs. The standard reference was immediately adjacent muscle tissue that was equidistant from the quadrature coil. The SI of the thrombus was assessed in its lengthwise central portion excluding the proximal and distal edges. The

Table 1
Experimental design

Time after venous thrombus initiation	4 h	1 week	2 weeks	4 weeks
Sequential MRI ($n=3$)	$n=3$	→	→	→
MRI and histological analysis ($n=12$)	$n=3$	$n=3$	$n=3$	$n=3$
MRI before and 30 min after t-PA ($n=24$)	$n=6$	$n=6$	$n=6$	$n=6$

T1 and T2 relaxation times were derived from the following respective equations: [17]

$$T_1 = \frac{TR}{\ln\left(\frac{\sin\alpha \cos\beta I_\beta - \sin\beta \cos\alpha I_\alpha}{\sin\alpha I_\beta - \sin\beta I_\alpha}\right)}$$

$$T_2 = \frac{TE_2 - TE_1}{\ln\left(\frac{I_1}{I_2}\right)}$$

2.4. Immunohistochemistry of rabbit venous thrombus

The jugular veins with thrombi were fixed in 4% paraformaldehyde for 24 h at 4°C, embedded in paraffin and sectioned (3 µm) for staining with hematoxylin and eosin (HE), Berlin blue (Fe³⁺) Sirius red (collagen) and with antibodies against platelet glycoprotein (GP) IIb/IIIa (Affinity Biologicals Inc., Ancaster, ON, Canada), rabbit fibrin (a gift from Takeda Chemical Industries, Ltd., Osaka, Japan), muscle actin (HHF35, DAKO, Glostrup, Denmark) and rabbit macrophages (RAM11, DAKO) [18]. The sections were then stained with Envision, anti-mouse IgG secondary antibody and horseradish peroxidase connected with a polymer (DAKO), or donkey anti-sheep IgG secondary antibody (Jackson ImmunoResearch, Inc., West Grove, PA, USA). Horseradish peroxidase activity was visualized using 3,3'-diaminobenzidine tetrahydrochloride, and the sections were faintly counterstained with Meyer's hematoxylin. Immunostaining controls included nonimmune mouse IgG or nonimmune sheep serum instead of the primary antibodies.

Areas of erythrocytes, iron, collagen and positive immunostaining in thrombi were analyzed using a color imaging morphometry system (Win Roof, Mitani, Fukui, Japan). Briefly, eosin-positive erythrocytes and Berlin-blue-positive, Sirius-red-positive or immunopositive areas were extracted using specific protocols based on the color parameters of hue, lightness and saturation. The data are expressed as ratios (%) of eosin-positive erythrocytes as well as Berlin-blue-positive, Sirius-red-positive or immunopositive regions in corresponding areas [19]. Two investigators who were blinded to the treatment assignments performed the morphological analyses.

2.5. Effect of t-PA infusion on whole blood coagulation parameters

Whole blood hemostatic parameters before and 30 min after t-PA administration (600,000 U/kg/h) were measured using a rotation thromboelastometry (ROTEM) analyzer (Pentapharm GmbH, Munich, Germany). Blood samples were collected from the central ear artery into 3.8% sodium citrate (9:1, vol/vol), and 300-µl portions were transferred into the ROTEM reaction chamber. Blood clotting was initiated using rabbit brain thromboplastin (ex-TEM, Pentapharm GmbH) and 20 µl of 200 mM CaCl₂, and then clot formation was measured in duplicate using the standard EXTEM evaluation parameters provided by the manufacturer.

We determined the following parameters: clotting time (CT), namely, the duration between recalcification and the start of clot formation; maximal clot firmness (MCF) (mm); and lysis onset time (LOT), namely, time at 75% MCF. These parameters describe the following phases of the clotting process: initiation (CT), termination/final clot strength (MCF) and fibrinolysis (LOT) [18].

2.6. Statistical analysis

All data are presented as medians and ranges, interquartile ranges or individual dots. Differences for individual groups were tested using the Mann–Whitney *U* test, the Wilcoxon signed rank test or the Kruskal–Wallis test with Dunn's multiple comparison test (GraphPad Prism 4.03, GraphPad Software Inc., San Diego, CA, USA). The degree of agreement was evaluated according to the Bland and Altman analysis (GraphPad).

3. Results

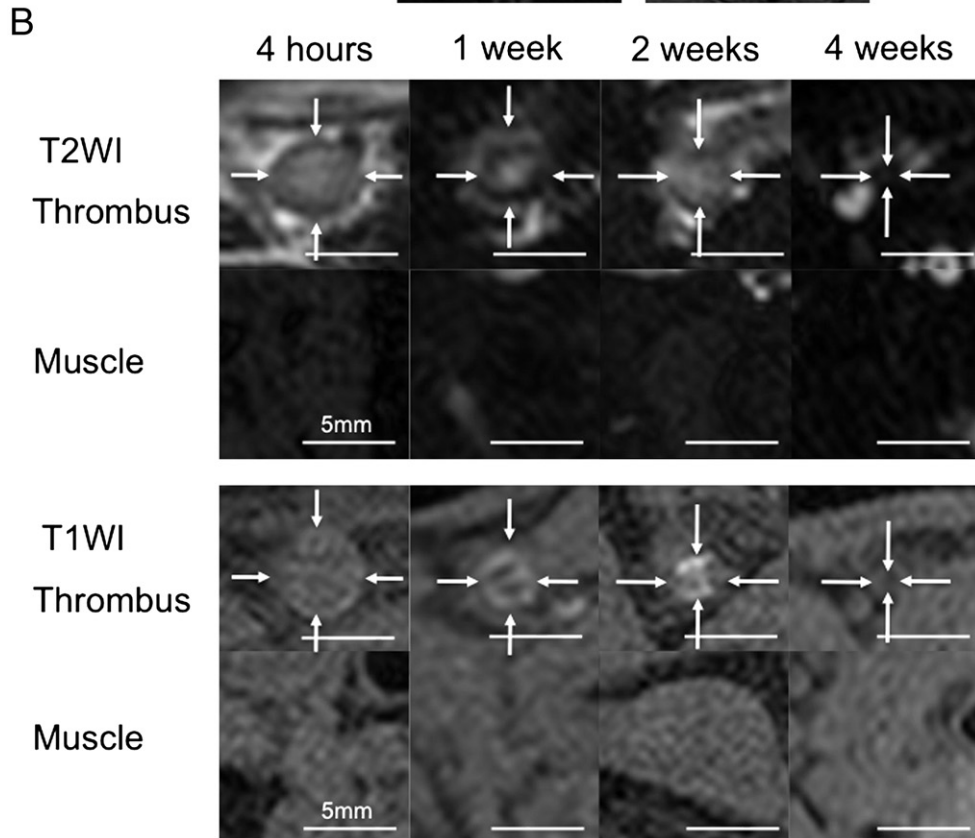
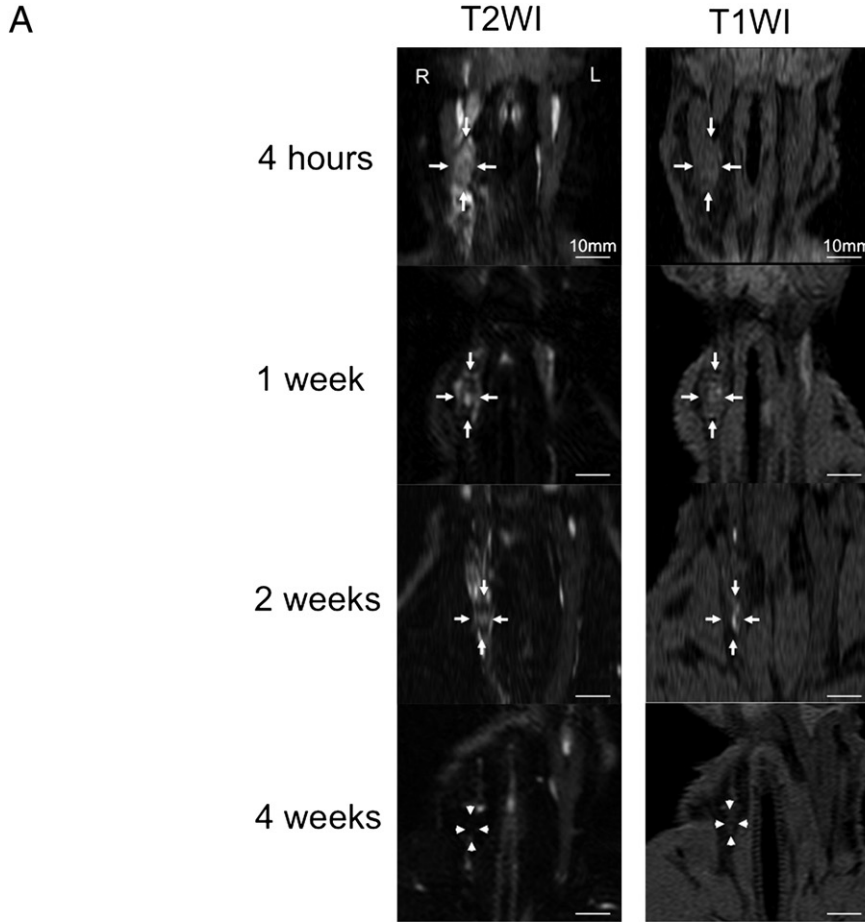
3.1. MRI of rabbit jugular vein

Figs. 1A and B show coronal and axial sequential MR images, respectively, of venous thrombi in the right jugular vein at 4 h and at 1, 2 and 4 weeks after endothelial denudation and vessel ligation. The thrombi at 4 h appeared as heterogeneous high or low SI on T2WI or T1WI, respectively, whereas those at 1 and 2 weeks appeared as heterogeneous high SI on both. The thrombi at 4 weeks appeared as homogeneous low SI on T2WI and T1WI. Figs. 1C to F show the SI values and relaxation times on axial images of venous thrombi at 4 h and at 1, 2 and 4 weeks. The T2WI SI time-dependently decreased, while T1WI SI increased in the thrombi at 1 and 2 weeks (Figs. 1C and D). The T2 and T1 relaxation times time-dependently decreased (Figs. 1E and F).

3.2. Pathological findings of venous thrombi

Fig. 2 shows thrombus areas determined by MR images or histological sections, and their Bland–Altman plot. The sizes of venous thrombi time-dependently decreased on MR images and in histological sections (Figs. 2A and B). The thrombi in MRI were comparable in size to histological sections (Fig. 2C).

To investigate the contents and organizing processes of thrombus, we histologically and immunohistologically examined sections of thrombi stained with hematoxylin–eosin, anti-GPIIb/IIIa, anti-fibrin, anti-muscle actin, anti-rabbit macrophage antibodies, Berlin blue and Sirius red. Fig. 3 shows the histological characteristics of the venous thrombi at 4 h and at 1, 2 and 4 weeks after the procedures. Thrombi at 4 h were rich in erythrocytes, platelets and fibrin without evidence of organization, indicating fresh thrombus. Thrombi at 1 and 2 weeks showed smooth muscle cell (SMC) proliferation and macrophage infiltration, as well as iron and collagen deposition at the thrombus–venous



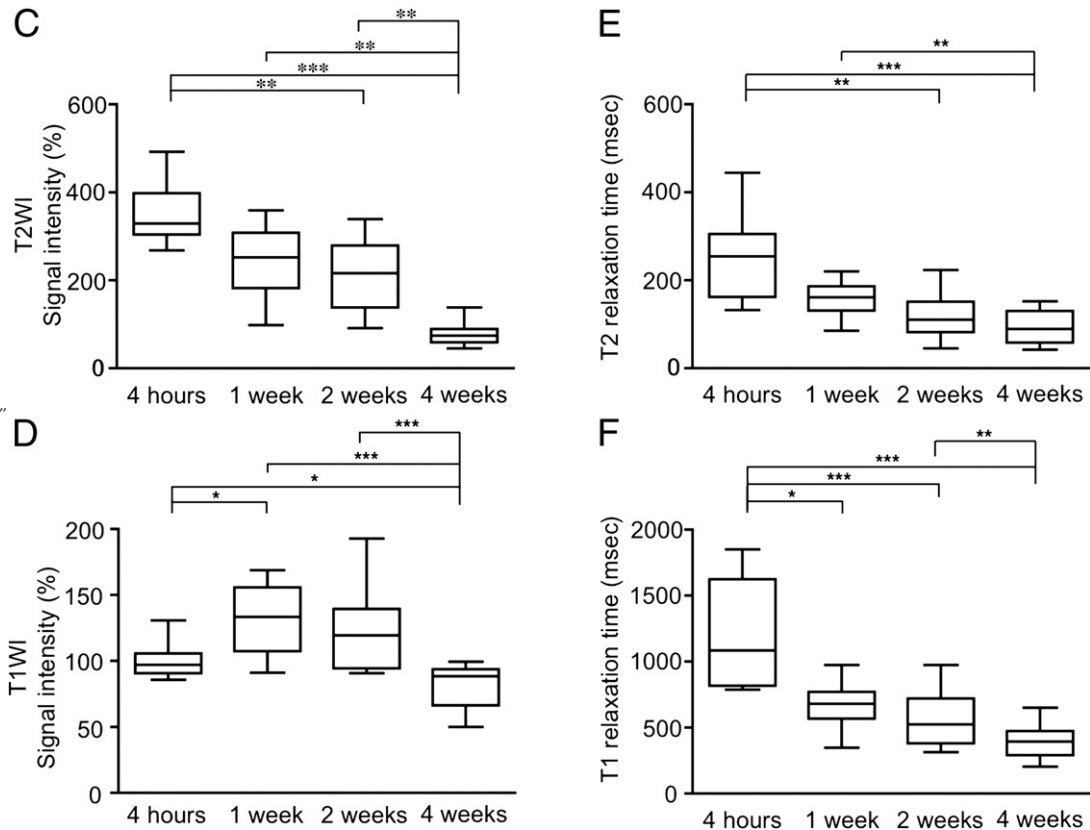


Fig. 1. Representative T2W and T1W MR images, signal intensities and relaxation times of venous thrombi induced in rabbit right jugular vein by endothelial denudation and vessel ligation. Sequential coronal MR images of venous thrombi (arrows) at 4 h and at 1, 2 and 4 weeks (A). Sequential axial MR images of venous thrombi (arrows) and reference adjacent muscle at the same times (B). Thrombi on T2WI or T1WI appeared as heterogeneous high or low SI, respectively, at 4 h, as heterogeneous high SI at 1 and 2 weeks and as homogeneous low SI at 4 weeks. Thrombus signal intensity changes over time of T2WI (C) and T1WI (D); * $P < .05$, ** $P < .01$, *** $P < .001$; $n = 18$ for each (Kruskal–Wallis test with Dunn’s multiple comparison test). Changes in T2 (E) and T1 (F) relaxation times of thrombi over time; * $P < .05$, ** $P < .01$, *** $P < .001$; $n = 18$ for each (Kruskal–Wallis test with Dunn’s multiple comparison test).

wall interface, indicating organizing thrombus. Thrombi at 4 weeks were replaced by fibrous connective tissue with SMCs, macrophages, collagen and small vessels. Iron was localized in macrophages, indicating hemosiderin deposition. The thrombi contained minimal erythrocytes, platelets and fibrin, indicating organized thrombus (Fig. 3A). Replacing primary antibodies with nonimmune mouse IgG did not elicit immunoreactivity (data not shown). Fig. 3B shows areas in thrombi of eosin-positive erythrocytes and those immunopositive and positive for Berlin blue and Sirius red at 4 h and at 1, 2 and 4 weeks. Semiquantitative analysis of the thrombi showed time-dependent decreases in areas of erythrocytes, platelets and fibrin; time-dependent increases in areas containing collagen and iron; and maximal amounts of SMC and macrophage infiltration at 2 weeks.

3.3. MRI of venous thrombi before and after t-PA administration

We examined the thrombolytic effects of t-PA upon venous thrombi at 4 h and at 1, 2 and 4 weeks using MRI. Whole blood clotting kinetics assessed using ROTEM showed obvious effects of t-PA. Both MCF and LOT sig-

nificantly decreased and shortened, respectively, indicating increased thrombolytic activity in the blood at 30 min after the administration of t-PA (Table 2). The administration of t-PA significantly decreased axial areas and thrombus volume at 4 h, but not at 1, 2 and 4 weeks (Figs. 4A, B and C).

4. Discussion

We showed here that MRI can reliably and noninvasively detect venous thrombi in rabbit jugular veins, that sequential changes in SI on T2WI and T1WI reflect organizing processes in these thrombi and that those with high SI on T2WI and low SI on T1WI respond to thrombolytic therapy.

Direct thrombus imaging using MR is a novel tool for diagnosing DVT with higher sensitivity and specificity than contrast venography [20,21], and MR could be superior to ultrasonography and computed tomography for the determination of DVT chronicity [22]. The present findings showed that MRI detected all thrombi created in rabbit jugular veins and that the thrombi in MR images were comparable in size to histological sections. In addition, the size of thrombi decreased throughout the organizing process. These findings

support the feasibility of diagnosing acute and chronic DVT by directly visualizing thrombus on MR images.

The SI of rabbit vein thrombi time-dependently decreased on T2WI, but increased on T1WI at 1 and 2 weeks after the procedure. These findings are in conflict with those of a study by Erdman et al. [14], who examined canine jugular veins using either T1- or T2-weighted spin echo sequences and a 0.35-T MR system. They found that the SI of the thrombi did not change over 3 weeks. Here, we used the spoiled gradient-recalled echo sequence and a 1.5-T MR system, which could be more sensitive to age-related changes in thrombi than the instruments used in the Erdman study. On the other hand, similar time-dependent changes occur in T2WIs and T1WIs of thrombi in swine or rabbit carotid arteries [23,24], but not in fresh thrombi; the SI in T2WIs could be high because fresh venous thrombi are rich in erythrocytes. Sequential changes could reflect the organizing processes of venous thrombi, as shown by histological analysis.

The heterogeneous appearance of thrombi in T1WI and T2WI might be due to their components, as well as to aging, namely, the organizing process, which includes progressive dehydration by fibrin gel, collagen production and hemosiderin depositions. The T1 and T2 relaxation times are positively affected by tissue water content and negatively affected by collagen and hemosiderin contents [25,26]. This could explain why T2 and T1 relaxation times that are high in fresh thrombi time-dependently decrease. Others have demonstrated that the proportion of oxy-, deoxy- and methemoglobin generated by erythrocyte degradation affects relaxation rates and MR images in vitro [27,28] and that changes in the proportion of hemoglobin contribute to age-related changes in MR signals in hematoma [29]. These findings suggest that methemoglobin formed in venous thrombi could contribute to the time-dependent decrease in T1 relaxation time. However, we found that T1 relaxation time shortened at 2 and 4 weeks in venous thrombi. Since the thrombi were rich in hemosiderin deposition and contained less erythrocytes, T1 relaxation time might be more influenced by hemosiderin than by methemoglobin. Changes in T2 and T1 relaxation times in venous thrombi could depend on a combination of sequential changes in the cellular and matrix components, the different oxygenation states of hemoglobin and hemosiderin deposition.

The administration of t-PA significantly decreased thrombus volume at 4 h, but not at 1, 2 and 4 weeks. Although how MR signals of venous thrombi respond to thrombolytic therapy is not clearly defined, Francis and Totterman [30] showed that human DVTs with a homogeneous low SI on T1WI were most likely to respond, whereas those with an intermediate or high intensity or a heterogeneous appearance do not. Our results suggest that venous thrombi with high and low SI on T2WI and T1WI, respectively, are likely to respond to thrombolytic therapy. Thrombolysis likely occurs in patients with symptomatic DVT of ≤ 4 days of duration and more often in partially than totally occluded segments [30]. Other clinical studies have also

found that the effect of thrombolytic therapy closely correlates with thrombus age, as reflected by the duration of clinical symptoms [8,31]. Our results support the notion that MRI can predict and assess the effects of thrombolytic therapy upon DVT.

The high accuracy of ultrasonography for diagnosis or exclusion of DVT in the thighs of symptomatic patients has been reported. However, the study can be difficult or limited in patients with obesity, marked swelling, overlying casts and pelvic DVT [6]. Several clinical studies were performed by using 2D TOF, phase-contrast (PC) or gadolinium-

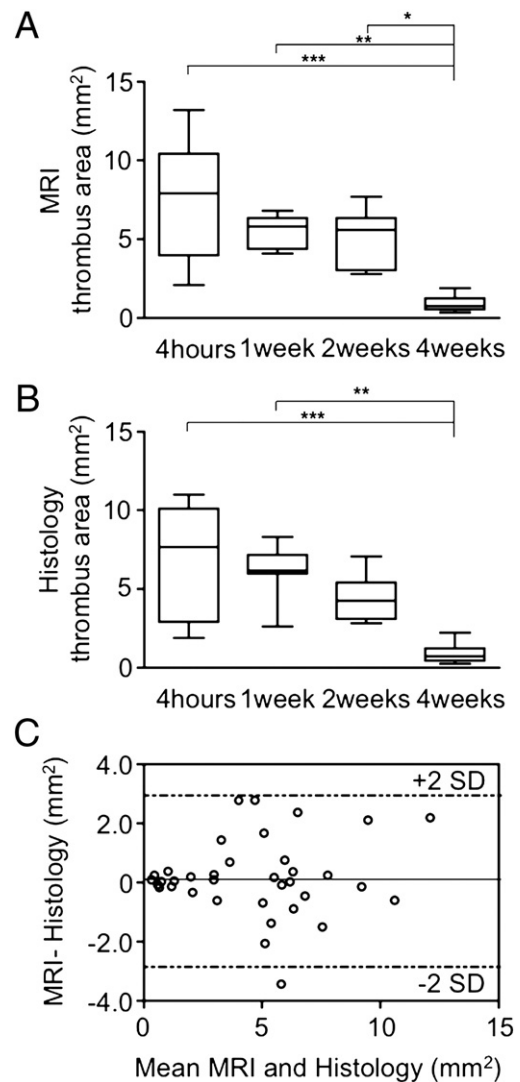


Fig. 2. Thrombus size in MR images and histological sections, and their Bland-Altman plot. Thrombus area in MR images ($n=9$ each) at 4 h and at 1, 2 and 4 weeks (A); * $P<.05$, ** $P<.01$, *** $P<.001$ (Kruskal–Wallis test with Dunn’s multiple comparison test). Thrombus area in histological sections ($n=9$ each) at 4 h and at 1, 2 and 4 weeks (B); * $P<.05$, ** $P<.01$, *** $P<.001$ (Kruskal–Wallis test with Dunn’s multiple comparison test). The thrombi in MR images were comparable in size to histological sections (Bland–Altman plot analysis, bias, 0.18 mm²; S.D., 1.29 mm²) (C). Bland–Altman limits (mean of the differences ± 2 S.D.s. of the differences) are shown.

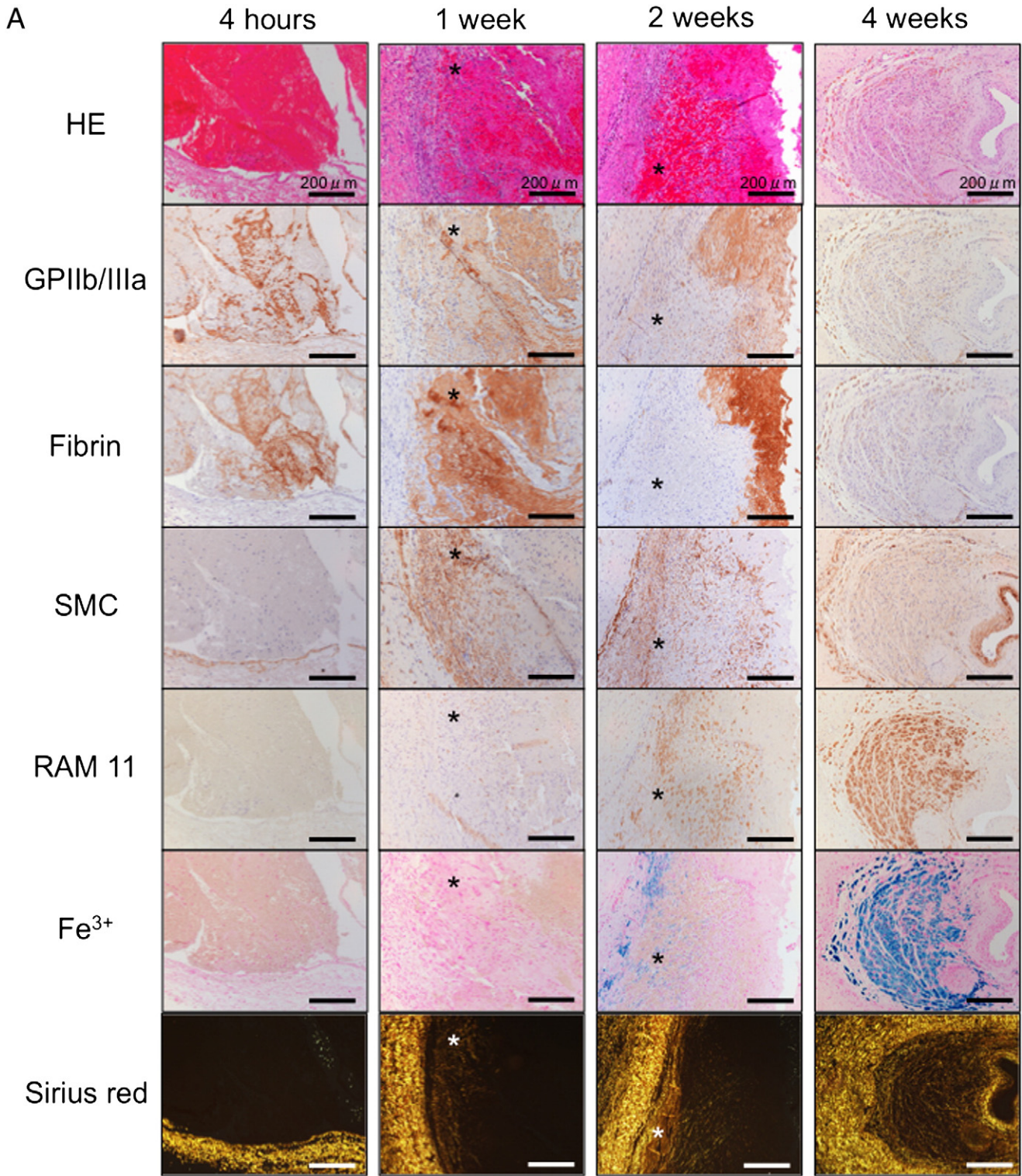


Fig. 3. Immunohistochemical microphotographs and immunopositive areas of venous thrombi at 4 h and at 1, 2 and 4 weeks after endothelial denudation and vessel ligation. Representative immunohistochemical microphotographs of fixed jugular veins containing thrombi that were stained with HE, anti-GPIIb/IIIa, anti-fibrin, anti-muscle actin, anti-rabbit macrophage antibodies, Berlin blue and Sirius red (A). Fresh venous thrombi at 4 h are rich in erythrocytes, platelets and fibrin without organization. Venous thrombi organizing at 1 and 2 weeks showed SMC proliferation, macrophage infiltration and iron and collagen deposition at thrombus–venous wall interface (*). Organized thrombi at 4 weeks are replaced by fibrous connective tissue with SMCs, iron-laden macrophages, collagen and small vessels. Changes in ratios of erythrocyte, platelet, fibrin, SMC, macrophage, Fe³⁺ and collagen areas in thrombi over time (B); * $P < .05$, ** $P < .01$, *** $P < .001$; $n = 9$ each (Kruskal–Wallis test with Dunn’s multiple comparison test).

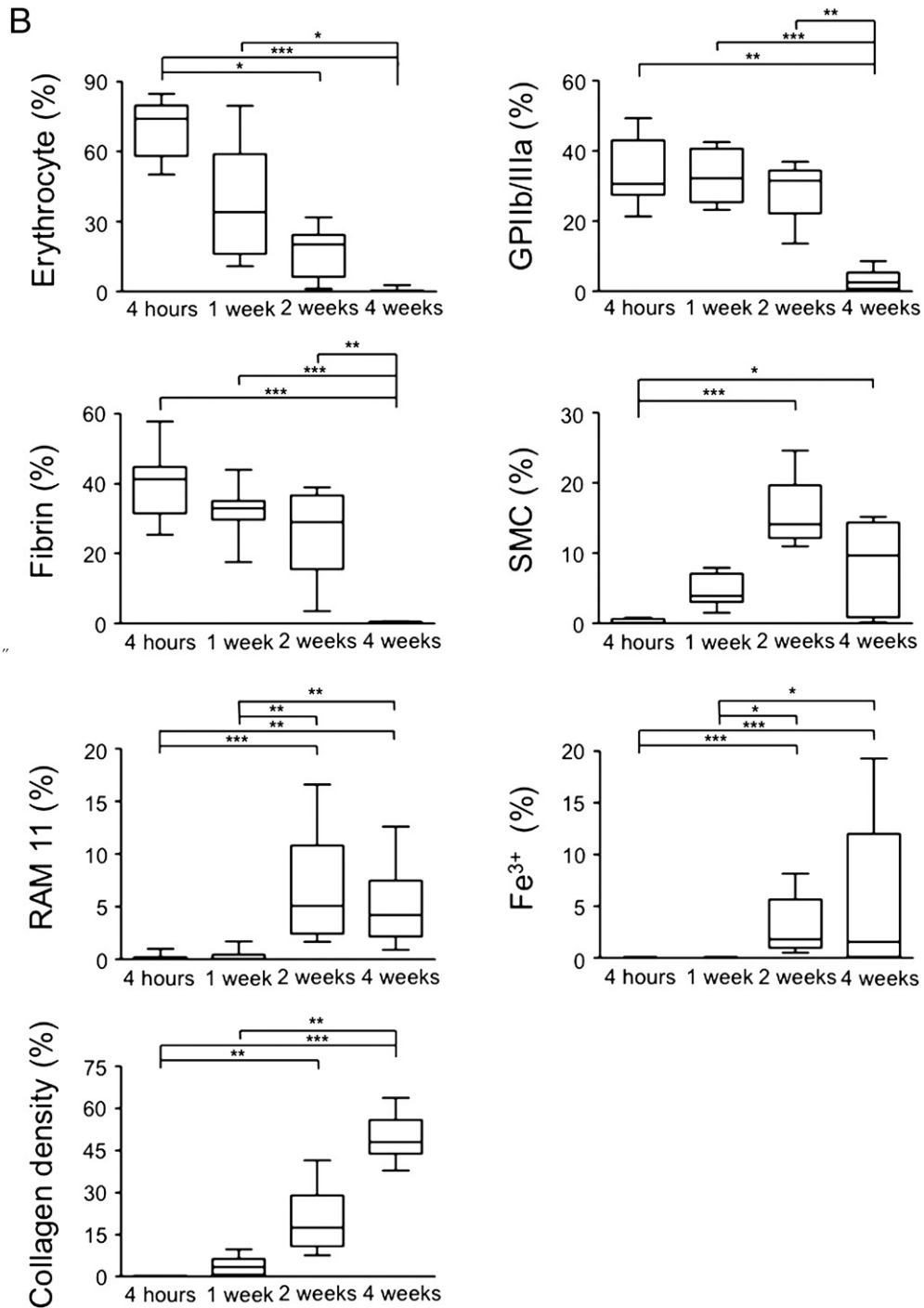


Fig. 3. (continued).

Table 2
Whole blood hemostatic parameters before and after t-PA administration

Parameter	Before t-PA	30 min after t-PA	P
	Median (range) n=6	Median (range) n=6	
CT (s)	62 (55–73)	56 (51–76)	.31
MCF (mm)	63 (59–68)	43 (24–57)	.03
LOT (s)	15,200 (9141–16,260)	331 (148–787)	.03

Data analyzed using Wilcoxon signed rank test.

enhanced MR angiography [32,33]. However, TOF and PC techniques are time consuming and are adversely affected by the slow, phasic flow that is typical for the peripheral venous system. The 3D FASE method combines the half-Fourier technique and 3D fast spin echo sequence. This method allows reduction of the imaging time with high spatial resolution. The 3D imaging has the inherent signal-to-noise ratio advantages, high resolution and isotropic voxels [34]. Therefore, the 3D FASE volumetric isotropic imaging data

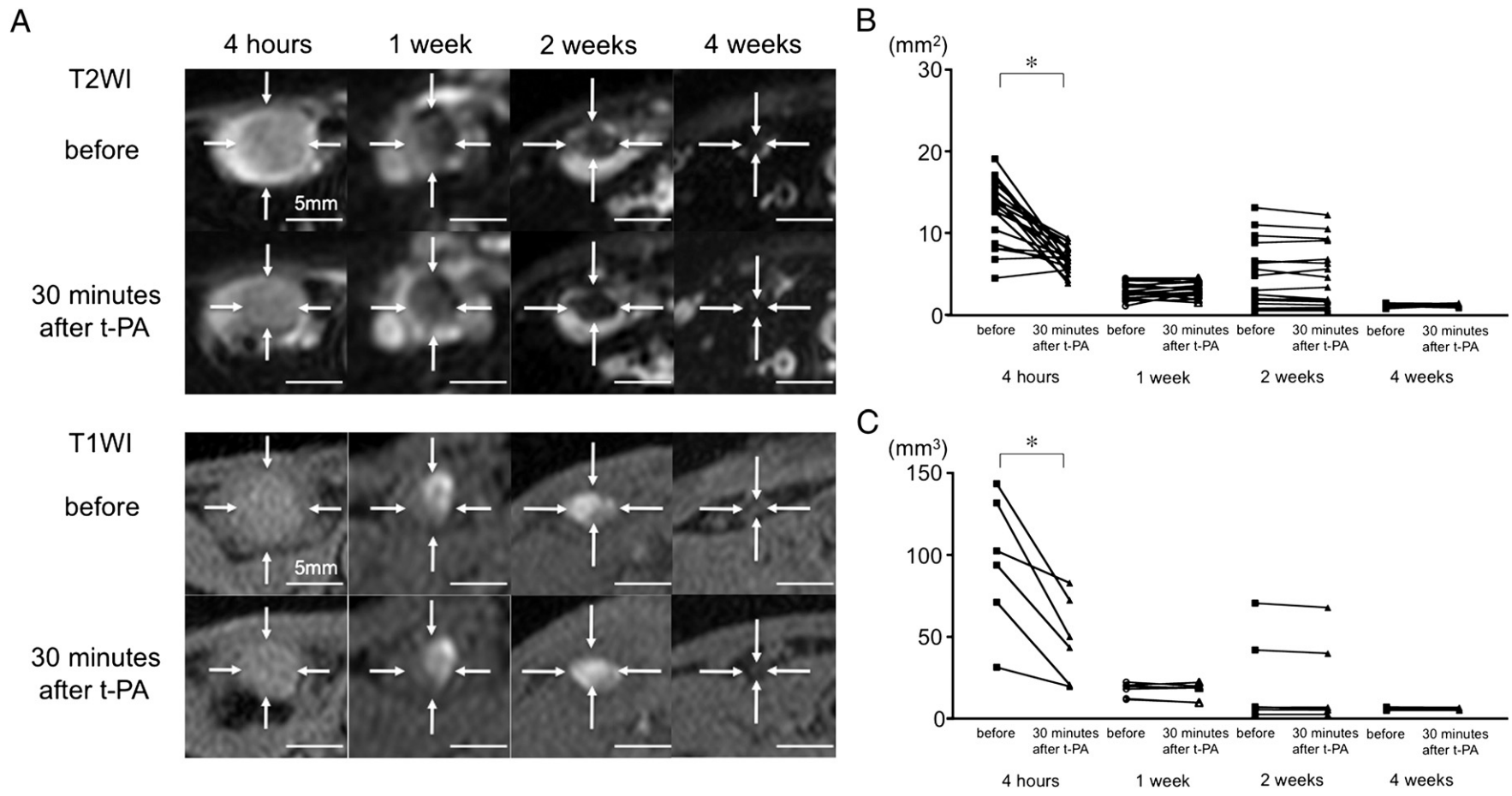


Fig. 4. Representative MR images and thrombus volume before and after t-PA administration. Representative axial MR images of venous thrombi before and 30 min after t-PA administration at 4 h and at 1, 2 and 4 weeks (A). Changes in axial area of thrombus before and 30 min after t-PA administration at 4 h and at 1, 2 and 4 weeks (B); $*P<.001$; $n=18$ per group (Wilcoxon signed rank test). Changes in thrombus volume before and 30 min after t-PA administration at 4 h and at 1, 2 and 4 weeks (C); $*P<.05$; $n=6$ per group (Wilcoxon signed rank test).

can be reformatted to generate high-quality, high-spatial-resolution images in any plane. Using the method, the present study detected sequential signal change of the venous thrombus over time and reduction of the thrombus size after t-PA administration. The 3D FASE might be a promising technique for DVT imaging.

5. Conclusion

Magnetic resonance imaging can reliably and noninvasively detect venous thrombosis, define thrombus age and predict as well as assess the thrombolytic response in rabbit veins. These results suggest that MRI shows promise as a diagnostic tool and as a means of predicting the effect of thrombolytic therapy on DVT.

References

- [1] Zhu T, Martinez I, Emmerich J. Venous thromboembolism: risk factors for recurrence. *Arterioscler Thromb Vasc Biol* 2009;29:298–310.
- [2] Takahashi M, Yamashita A, Moriguchi-Goto S, et al. Critical role of von Willebrand factor and platelet interaction in venous thromboembolism. *Histol Histopathol* 2009;24:1391–8.
- [3] Sugita C, Yamashita A, Moriguchi-Goto S, et al. Factor VIII contributes to platelet-fibrin thrombus formation via thrombin generation under low shear conditions. *Thromb Res* 2009;124:601–7.
- [4] Sigel B, Swami V, Can A, et al. Intimal hyperplasia producing thrombus organization in an experimental venous thrombosis model. *J Vasc Surg* 1994;19:350–60.
- [5] Usui Y, Sauvage LR, Wu HD, et al. A comparative experimental study of the organization of arterial and venous thrombi. *Ann Surg* 1987;205:312–7.
- [6] Katz DS, Hon M. Current DVT imaging. *Tech Vasc Interv Radiol* 2004;7:55–62.
- [7] Marder VJ, Sherry S. Thrombolytic therapy: current status (1). *N Engl J Med* 1988;318:1512–20.
- [8] Francis CW, Marder VJ. Fibrinolytic therapy for venous thrombosis. *Prog Cardiovasc Dis* 1991;34:193–204.
- [9] Evans AJ, Crisp AJ, Colville A, et al. Pulmonary infections caused by *Mycobacterium malmoense* and *Mycobacterium tuberculosis*: comparison of radiographic features. *AJR Am J Roentgenol* 1993;161:733–7.
- [10] Polak JF, Fox LA. MR assessment of the extremity veins. *Semin Ultrasound CT MR* 1999;20:36–46.
- [11] Laissy JP, Cinqualbre A, Loshkajian A, et al. Assessment of deep venous thrombosis in the lower limbs and pelvis: MR venography versus duplex Doppler sonography. *AJR Am J Roentgenol* 1996;167:971–5.
- [12] Dupas B, el Kouri D, Curtet C, et al. Angiomagnetic resonance imaging of iliofemorocaval venous thrombosis. *Lancet* 1995;346:17–9.
- [13] Enden T, Storås TH, Negård A, et al. Visualization of deep veins and detection of deep vein thrombosis (DVT) with balanced turbo field echo (b-TFE) and contrast-enhanced T1 fast field echo (CE-FFE) using a blood pool agent (BPA). *J Magn Reson Imaging* 2010;31:416–24.
- [14] Erdman WA, Weinreb JC, Cohen JM, et al. Venous thrombosis: clinical and experimental MR imaging. *Radiology* 1986;161:233–8.
- [15] Takahashi M, Yamashita A, Moriguchi-Goto S, et al. Inhibition of factor XI reduces thrombus formation in rabbit jugular vein under endothelial denudation and/or blood stasis. *Thromb Res* 2010;125:464–70.
- [16] Du YP, Parker DL, Davis WL, et al. Reduction of partial-volume artifacts with zero-filled interpolation in three-dimensional MR angiography. *J Magn Reson Imaging* 1994;4:733–41.
- [17] Kuroiwa Y, Yamashita A, Miyati T, et al. Atherosclerotic lesions rich in macrophages or smooth muscle cells discriminated in rabbit iliac arteries based on T1 relaxation time and lipid content. *Acad Radiol* 2010;17:230–8.
- [18] Yamashita A, Matsuda S, Matsumoto T, et al. Thrombin generation by intimal tissue factor contributes to thrombus formation on macrophage-rich neointima but not normal intima of hyperlipidemic rabbits. *Atherosclerosis* 2009;206:418–26.
- [19] Yamashita A, Shoji K, Tsuruda T, et al. Medial and adventitial macrophages are associated with expansive atherosclerotic remodeling in rabbit femoral artery. *Histol Histopathol* 2008;23:127–36.
- [20] Moody AR, Pollock JG, O'Connor AR, et al. Lower-limb deep venous thrombosis: direct MR imaging of the thrombus. *Radiology* 1998;209:349–55.
- [21] Fraser DG, Moody AR, Morgan PS, et al. Diagnosis of lower-limb deep venous thrombosis: a prospective blinded study of magnetic resonance direct thrombus imaging. *Ann Intern Med* 2002;136:89–98.
- [22] Spritzer CE, Trotter P, Sostman HD. Deep venous thrombosis: gradient-recalled-echo MR imaging changes over time — experience in 10 patients. *Radiology* 1998;208:631–9.
- [23] Corti R, Osende JJ, Fayad ZA, et al. In vivo noninvasive detection and age definition of arterial thrombus by MRI. *J Am Coll Cardiol* 2002;39:1366–73.
- [24] Sirol M, Fuster V, Badimon JJ, et al. Chronic thrombus detection with in vivo magnetic resonance imaging and a fibrin-targeted contrast agent. *Circulation* 2005;112:1594–600.
- [25] Scholz TD, Fleagle SR, Burns TL, et al. Tissue determinants of nuclear magnetic resonance relaxation times. Effect of water and collagen content in muscle and tendon. *Invest Radiol* 1989;24:893–8.
- [26] Vymazal J, Urgosik D, Bulte JW. Differentiation between hemosiderin- and ferritin-bound brain iron using nuclear magnetic resonance and magnetic resonance imaging. *Cell Mol Biol* 2000;46:835–42.
- [27] Clark RA, Watanabe AT, Bradley Jr WG, et al. Acute hematomas: effects of deoxygenation, hematocrit, and fibrin-clot formation and retraction on T2 shortening. *Radiology* 1990;175:201–6.
- [28] Bryant RG, Marill K, Blackmore C, et al. Magnetic relaxation in blood and blood clots. *Magn Reson Med* 1990;13:133–44.
- [29] Bradley Jr WG. MR appearance of hemorrhage in the brain. *Radiology* 1993;189:15–26.
- [30] Francis CW, Totterman S. Magnetic resonance imaging of deep vein thrombi correlates with response to thrombolytic therapy. *Thromb Haemost* 1995;73:386–91.
- [31] Theiss W, Wirtzfeld A, Fink U, et al. The success rate of fibrinolytic therapy in fresh and old thrombosis of the iliac and femoral veins. *Angiology* 1983;34:61–9.
- [32] Spritzer CE, Arata MA, Freed KS. Isolated pelvic deep venous thrombosis: relative frequency as detected with MR imaging. *Radiology* 2001;219:521–5.
- [33] Hoffmann U, Loewe C, Bernhard C, et al. MRA of the lower extremities in patients with pulmonary embolism using a blood pool contrast agent: initial experience. *J Magn Reson Imaging* 2002;15:429–37.
- [34] Yang D, Kodama T, Tamura S, et al. Evaluation of the inner ear by 3D fast asymmetric spin echo (FASE) MR imaging: phantom and volunteer studies. *Magn Reson Imaging* 1999;17:171–82.